

DOI: 10.19884/j.1672-5220.202404010

# Intelligent Metal Detection and Disposal Automation Equipment Based on Geometric Optimization Driving Algorithm

TIAN Xuehui, LI Chengzu, WEI Kehan, QIAN Yang, ZHANG Lu, WANG Rongwu\*

College of Textiles, Donghua University, Shanghai 201620, China

**Abstract:** In order to solve the problem of metal impurities mixed in the production line of wood pulp nonwoven raw materials, intelligent metal detection and disposal automation equipment is designed. Based on the principle of electromagnetic induction, the precise positioning of metal coordinates is realized by initial inspection and multi-directional re-inspection. Based on a geometry optimization driving algorithm, the cutting area is determined by locating the center of the circle that covers the maximum area. This approach aims to minimize the cutting area and maximize the use of materials. Additionally, the method strives to preserve as many fabrics at the edges as possible by employing the farthest edge covering circle algorithm. Based on a speed compensation algorithm, the flexible switching of upper and lower rolls is realized to ensure the maximum production efficiency. Compared with the metal detection device in the existing production line, the designed automation equipment has the advantages of higher detection sensitivity, more accurate metal coordinate positioning, smaller cutting material areas and higher production efficiency, which can make the production process more continuous, automated and intelligent.

**Key words:** intelligent manufacturing; electromagnetic induction; metal detection; geometric optimization driving algorithm; automation equipment

CLC number: TP23

Document code: A

Article ID: 1672-5220(2024)05-0492-13

Open Science Identity  
(OSID)



## 0 Introduction

Industry 4.0, focusing on intelligent and networked manufacturing systems, has been incorporated into the national “14th Five-Year Plan” and has become the core strategy to promote the fundamental transformation of the manufacturing industry<sup>[1-2]</sup>. The medical nonwoven industry, as a key area directly related to public health and personal health, plays a core role in many important fields such as disease prevention and environmental protection. However, the industry is currently facing the dual challenges of high labor costs and insufficient

automation. The solution to these problems is crucial to improving the efficiency and the market competitiveness of the industry. In the weaving industry, it is particularly necessary to transform the production process into a more continuous, automated and intelligent operation mode. This transformation can not only significantly enhance the production efficiency and reduce operating costs, but also ensure the product quality and meet the high standards of high efficiency, high flexibility and intelligent production in the era of Industry 4.0, thus promoting the continuous progress and technological innovation of the medical nonwoven industry<sup>[3-5]</sup>.

Metal detection devices have been applied in more and more areas, such as agricultural harvesting, glass production, coal transportation, airports, banks, food processing, textile production and pharmaceutical production<sup>[6]</sup>. There are many kinds of metal detection technologies. For example, Yang et al.<sup>[7]</sup> used an X-ray fluorescence spectrometer to determine 10 metal elements (arsenic, barium, cobalt, chromium, copper, manganese, nickel, lead, vanadium and zinc) in soil. The operation is convenient and fast, and the accuracy is high. The X-ray metal detection technology can accurately distinguish metal, glass, liquid and other non-metallic items, but there is a certain amount of electromagnetic radiation. The electromagnetic radiation emitted by X-rays for a long time will be harmful to the human body, the cost of an X-ray fluorescence spectrometer is expensive, and its application is limited. Jiang et al.<sup>[8]</sup> used a microwave detection technology to determine the content of heavy metal Pb in soybean oil. The principle is to distinguish metals by using the different perception effects of metal objects on physical phenomena, for example ultrasound. Although the application range of the microwave detection technology is relatively limited, it has great advantages in metal crack detection<sup>[9]</sup>. The most widely used metal detection device in the material production line is the electromagnetic induction type which judges the existence of the metal by detecting the alternating current generated by the metal in the magnetic field<sup>[10]</sup>. However, there are

Received date: 2024-04-15

Foundation items: National Key Research and Development Program of China (Nos. 2022YFB4700600 and 2022YFB4700605)

\* Correspondence should be addressed to WANG Rongwu, email: wrw@dhu.edu.cn

Citation: TIAN X H, LI C Z, WEI K H, et al. Intelligent metal detection and disposal automation equipment based on geometric optimization driving algorithm[J]. *Journal of Donghua University (English Edition)*, 2024, 41(5): 492-504.

also some problems. In addition to low sensitivity<sup>[11]</sup>, only metal targets can be detected. Once metal impurities are detected, all materials on the production line are immediately abolished and cannot be accurately positioned. In addition, the machine must be shut down when the metal impurities are removed, which seriously affects the production efficiency. In the actual production, the wood pulp roll is unwound and enters the opening machine through the conveying device. After fully opening, it is mixed with other raw materials, and then the new product can be obtained after the specific treatment process. If mixed with metal impurities, when the wood pulp roll is opened, it will rub and collide with the internal hitters, causing damage to the production equipment. The wood pulp is a flammable material, and the friction spark may cause fire. In the whole production process of making wood pulp rolls, it is possible to mix rectangular, circular and irregular metal debris. Therefore, it is significant to design an automatic equipment with high sensitivity, which can accurately detect the metal impurities in the wood pulp roll and remove them in time before transported into the opening machine.

In this research, an intelligent metal detection and disposal automation equipment based on a geometric optimization driving algorithm is designed. Eddy current sensors and self-oscillating detection circuits are applied, and the arrangement of detection coils is optimized, which would effectively improve the speed of metal detection. After a series of circuit design, the metal detection sensitivity is tested and adjusted according to the needs of the production line, and the LED light is driven to realize the initial positioning of the metal impurity. The metal detection device moves freely along the  $X$  axis and the  $Y$  axis, and performs multi-directional secondary detection on the wood pulp roll. By analyzing the signal peak of the detection coil, the precise positioning of the metal impurity coordinates is realized.

The research integrates a geometric optimization driving algorithm to identify the cutting area for removing metal impurities, focusing on minimizing the disruption to the wood pulp roll. By identifying the center of a circle that encompasses the largest number of metal flaws, the algorithm aims to optimize the removal process, ensuring the maximum material retention and efficiency. This approach, especially the application of the farthest edge covering circle algorithm, is crucial for preserving as much of the roll edge as possible, thereby maintaining the roll structural integrity and avoiding issues during edge grinding and transport.

After determining the central coordinates of the most flaw-dense area and the subsequent cutting zone using the geometric optimization driving algorithm, the device methodically removes the detected contaminants. Furthermore, the study delves into a speed compensation algorithm to enable smooth transitions between different wood pulp rolls, ensuring the accurate extraction of metal

contaminants and the seamless operation of subsequent processes, thereby enhancing the overall production efficiency.

## 1 Principle of Operation

### 1.1 Eddy current sensor

The eddy current sensor uses the eddy current effect<sup>[12]</sup> to convert non-electric quantities such as displacements and temperatures into changes in the impedance (or changes in the inductance, or changes in the quality factor  $Q$ ), thereby performing non-electric quantity measurement.

As shown in Fig. 1, due to the change of the current, an alternating magnetic field  $H_1$  is generated around a sensor coil with an alternating current  $I_1$ . When the measured conductor is placed within the range of the magnetic field, the measured conductor internally generates the eddy current  $I_2$ . The eddy current will also produce a new magnetic field  $H_2$  that is opposite to  $H_1$ , thus offsetting part of the original magnetic field, resulting in changes in the impedance, the inductance and the quality factor of the sensor coil.

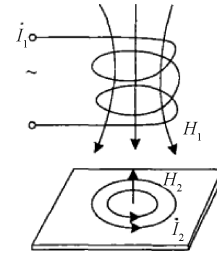


Fig. 1 Principle diagram of eddy current sensor

The changes of the impedance, the inductance and the quality factor of the sensor coil are related to the geometry, the conductivity and the permeability of the conductor, as well as the geometry of the sensor coil, the frequency of the current, and the distance between the sensor coil and the measured conductor. If only one of the above parameters changes, various sensors for measuring displacements, temperatures, hardness and so on can be formed.

### 1.2 Self-oscillating detection circuit

Most of the self-oscillating metal detectors use an inductance capacitor (LC) oscillator as the detection circuit of metal objects<sup>[13]</sup>. The LC oscillator is widely used in factories or mines. The detection circuit is shown in Fig. 2.

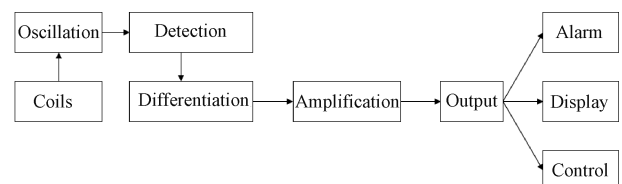


Fig. 2 Self-oscillating detection circuit

The oscillator outputs an equal amplitude alternating current (AC) voltage under normal conditions, and after detection, it is a constant direct current (DC) voltage. Thus the output differential signal is zero. When the metal object passes through the sensor coil, the amplitude of the oscillator decreases and then recovers. The DC voltage after detection produces a reduced fluctuation. After differential circuit processing, a pulse signal will be output. After the pulse signal is amplified by the amplifier, the relay is driven to act, and the contact signal is output to control the metal removal device.

## 2 Optimization of Coil Arrangement

### 2.1 Two coil combinations

The arrangement of two coil combinations is shown in Fig. 3. The two detection coils are placed in parallel in the longitudinal direction and connected in series with each other as a small detection area.



Fig. 3 Two coil combination

The electromagnetic interference between two adjacent small detection areas is small, and the positioning of metal impurities is accurate. However, due to the large number of coils, the number of extracted signals is large, resulting in more complex follow-up processing. The magnetic field intensity is small, and the recognition rate of metal impurities is reduced.

### 2.2 Four coil combinations

The arrangement of four coil combinations is shown in Fig. 4. The four detection coils are divided into two rows, arranged in parallelograms and connected in series as a small detection area.



Fig. 4 Four coil combination

This combination produces a strong magnetic field, a high detection rate of metal impurities and a small number of signals to be extracted, and the subsequent processing is simple. However, the electromagnetic interference at the junction of two adjacent small detection areas is large, which affects the accurate removal of subsequent metal impurities.

### 2.3 Three coil combinations

The arrangement of three coil combinations is shown in Fig. 5. On the basis of the four coil combination, one coil is removed at the junction of adjacent small detection areas. The three coils are arranged in triangles and connected in series with each other as a small detection area.

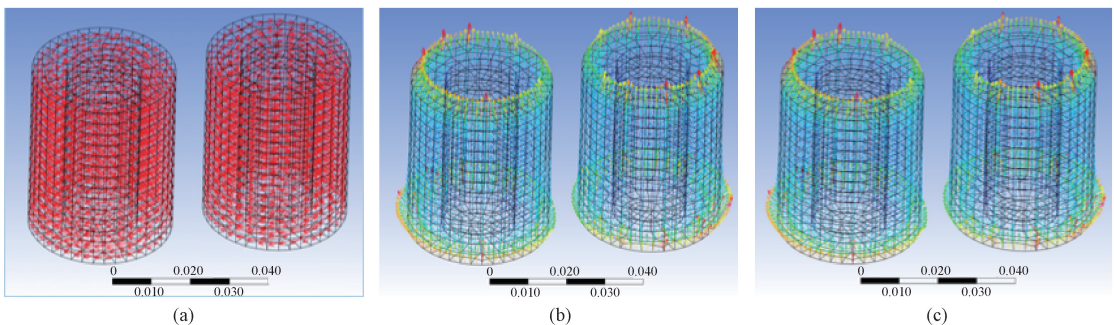


Fig. 5 Three coil combination

This combination can effectively reduce the electromagnetic interference between adjacent small detection areas. The metal impurity positioning range is moderate, the magnetic field is strong, the metal detection rate is high, the number of signals to be extracted is small, and the subsequent processing is simple.

### 2.4 Static magnetic simulation analyses

The static magnetic simulation analyses of two coil combinations, three coil combinations and four coil combinations are carried out by ANSYS Workbench. The outer diameter of each coil is 37 mm, the inner diameter is 19 mm, the iron core diameter is 19 mm, the coil turns are 50, the conductive area is  $5 \times 10^{-4} \text{ m}^2$ , the maximum current density is  $5 \times 10^4 \text{ A/m}^2$ , the frequency is 25 kHz, and the center distance between two coils is 45 mm. The results of the current density, the total magnetic flux density and the total magnetic field intensity are obtained. The static magnetic simulation analyses are shown in Fig. 6. The average values of the current density, the total magnetic flux density and the total magnetic field intensity are shown in Table 1.



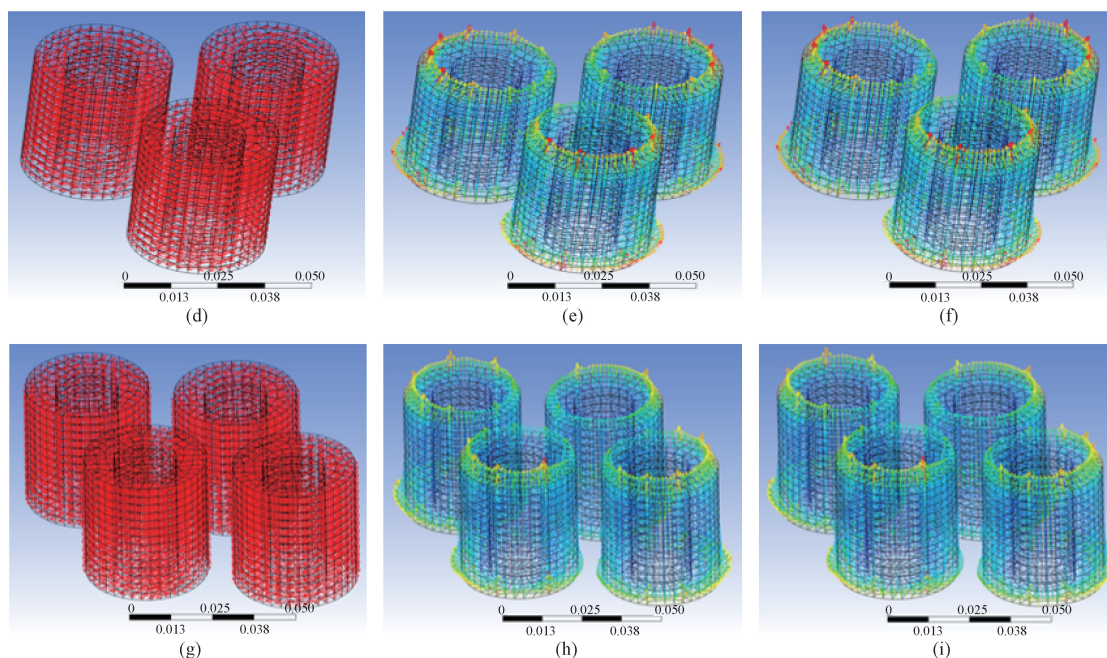


Fig. 6 Static magnetic simulation analyses(unit: m): (a) current density diagram of two coil combinations; (b) total magnetic flux density diagram of two coil combinations; (c) total magnetic field intensity diagram of two coil combinations; (d) current density diagram of three coil combinations; (e) total magnetic flux density diagram of three coil combinations; (f) total magnetic field intensity diagram of three coil combinations; (g) current density diagram of four coil combinations; (h) total magnetic flux density diagram of four coil combinations; (i) total magnetic field intensity diagram of four coil combinations

**Table 1** Static magnetic simulation analysis results of different numbers of coil combinations

Method	Current density/( $A/m^2$ )	Total magnetic flux density/T	Total magnetic field intensity/( $A/m$ )
Two coil combinations	181.790	$1.086 \times 10^{-4}$	86.409
Three coil combinations	179.770	$1.012 \times 10^{-4}$	80.527
Four coil combinations	157.070	$8.709 \times 10^{-5}$	69.302

It can be seen from Table 1 that with the increase of the number of coil combinations, although the number of extracted signals decreases and the subsequent processing is simple, the average values of the current density, the total magnetic flux density and the total magnetic field intensity gradually decrease, which leads to the decrease of the metal detection sensitivity. Compared with two coil combinations, the average values of three coil combinations decrease less, the total magnetic field intensity changes less, and the metal detection sensitivity is less affected. The average values of four coil combinations decrease greatly, and the total magnetic field intensity is obviously weakened, resulting in a significant reduction in the metal detection sensitivity.

In summary, the arrangement of three coil combinations is more advantageous. The magnetic field is strong, the metal detection sensitivity is high, the number of extracted signals can be reduced, and the subsequent processing is convenient. The triangle configuration can also take more efficient use of space, especially when multiple detection coils are deployed in a limited space.

### 3 Circuit Design

The permanent magnet and the detection coil in the detection probe form a working magnetic field. When metal impurities enter the detection area, they will cause changes in the local magnetic field environment, and will cause fluctuations in the instantaneous current of the local magnetic field. The perceived abnormal current is converted into a voltage signal. After the OP07 precision operational amplifier performs voltage tracking and differential amplification, the eight-way voltage signal is input into the CD4051BM96 analog multiplexer, and the output signal with metal impurities is selected. The voltage signal is filtered by the voltage regulator, input into the TP27-SR comparator, and compared with the detection sensitivity voltage threshold set by the X9C104 digital potentiometer. If the voltage signal reaches or exceeds the set threshold, the TL0721 signal amplifier further amplifies the detection signal and inputs it into the C8051F500 single-chip microcomputer to drive the LED light and the metal impurity removal device.

### 3.1 Differential amplification and signal selection

The metal detection probe is divided into upper and lower groups. Each detection position is composed of three probe coils (signal 1 and signal 2) of group 1 and group 2, and up to eight large detection positions can be detected. The two groups of signals can be monitored by the internal comparator of the C8051F500 single-chip microcomputer, and the pins are P2.7 and P3.0.

The two detection signals (signal 1 and signal 2) at one detection position are analyzed, and the others are the same. Signal 1 and signal 2 are first followed by two OP07 precision operational amplifiers for voltage tracking<sup>[14]</sup>, and then are differential amplified by one OP07 precision

operational amplifier (shown in Fig. 7). In order to save CPU resources, the CD4051BM96 analog multiplexer is adopted. It is an eight-channel analog/digital multiplexer switch<sup>[15]</sup>. Pins 1, 2, 4, 5, 12, 13, 14 and 15 are the input/output terminals; pins 9, 10 and 11 are the address terminals; the pin 3 is the common output/input terminal; the pin 6 is the forbidden terminal; the pin 7 is the negative voltage terminal; the pin 8 is the digital signal grounding terminal; the pin 16 is the positive voltage terminal. By controlling the address and the chip selection signal of the CD4051BM96 analog multiplexer, the single-chip microcomputer selects a signal for output for the subsequent circuit processing (shown in Fig. 8).

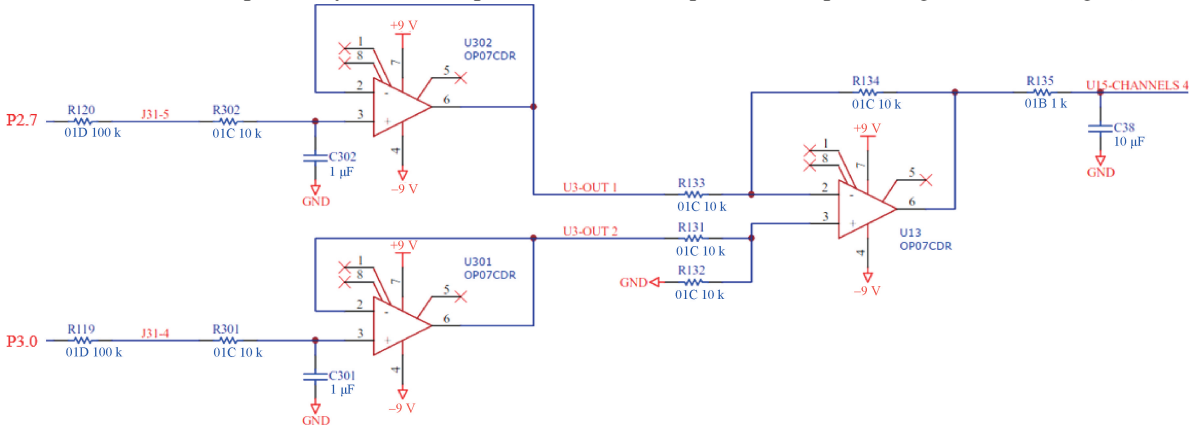


Fig. 7 Differential amplifier circuit

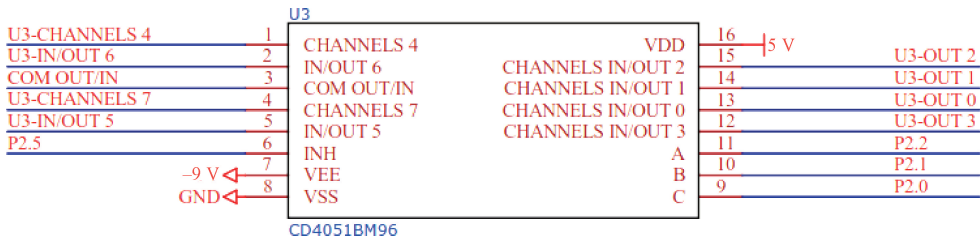


Fig. 8 Signal selection circuit

### 3.2 Sensitivity adjustment

The X9C104 digital potentiometer uses pins P1.4, P1.5 and P1.6 to communicate with the C8051F500 single-chip microcomputer, and realizes the adjustment function of the internal variable resistance according to the regular high and low levels received by the three pins (shown in Fig. 9). The pin P1.6 is the chip selection signal, and when the input is at a low level, the chip is enabled; the pin P1.5 can adjust the potentiometer at the falling edge; the pin P1.4 is set high to represent an increase in resistance and set low to represent a decrease in resistance. VH/RH is the upper end of the internal sliding resistance, and the voltage that needs to be divided is connected; VL/RL is the lower end of the internal sliding resistance; VW/RW is the variable middle end of the internal sliding resistance, and the voltage after the adjustment resistance is output. The X9C104 digital potentiometer is connected with the TP27-SR comparator. By controlling the C8051F500 single-chip microcomputer,

the internal variable resistance of the X9C104 digital potentiometer, the output voltage and the single-ended voltage of the comparator can be adjusted to realize the adjustment of the metal detection sensitivity.

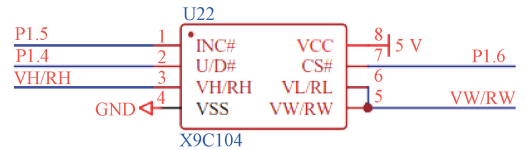


Fig. 9 Sensitivity adjustment circuit

### 3.3 Regulated filtering

Through the B0505S-1WR2 isolated power supply (shown in Fig. 10), the L78M09ABDT-TR linear regulator (shown in Fig. 11), the NJM79M09DL1A negative voltage regulator (shown in Fig. 12) and the corresponding voltage stabilizing filter circuits, voltages of 5, 9, 12, -12 and -9 V can be obtained.

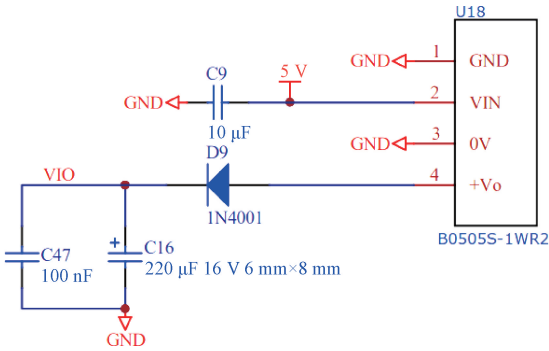


Fig. 10 B0505S-1WR2 isolated power supply and voltage stabilizing filter circuit

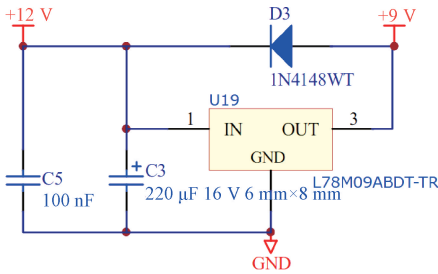


Fig. 11 L78M09ABDT-TR linear regulator and voltage stabilizing filter circuit

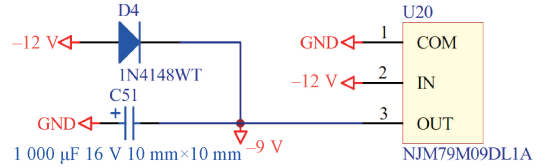


Fig. 12 NJM79M09DL1A negative voltage regulator and voltage stabilizing filter circuit

### 3.4 Threshold comparison and signal amplification

Through the TP27-SR comparator, the detection signal selected by the CD4051BM96 analog multiplexer is compared with the detection sensitivity set by the X9C104 digital potentiometer (shown in Fig. 13). When the detection signal reaches or exceeds the set voltage threshold, the TL0721 signal amplifier further amplifies the detection signal and inputs it into the C8051F500 single-chip microcomputer (shown in Fig. 14) to drive the LED light and the metal impurity removal device.

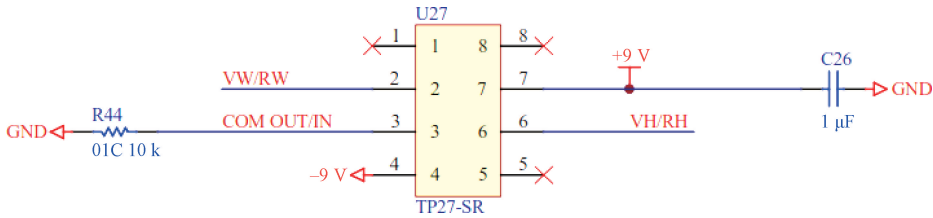


Fig. 13 Threshold comparison circuit

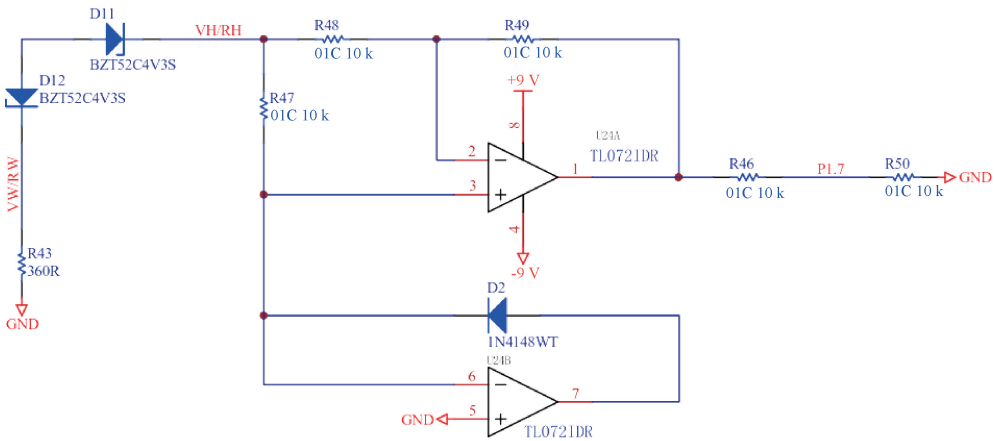


Fig. 14 Signal amplifying circuit

### 3.5 LED light driver

When metal impurities are detected, the LED light (LED display) corresponding to the detection position is turned on. The LED light can be driven by the C8051F500 single-chip microcomputer<sup>[16]</sup> (shown in Fig. 15) and TM1618 (shown in Fig. 16). TM1618 is a

special circuit for LED light drive control with keyboard scanning interface. It integrates microcomputer digital interface, data latch, LED light high voltage drive, keyboard scanning and other circuits. The operation panel is communicated through the serial port of the single-chip microcomputer.

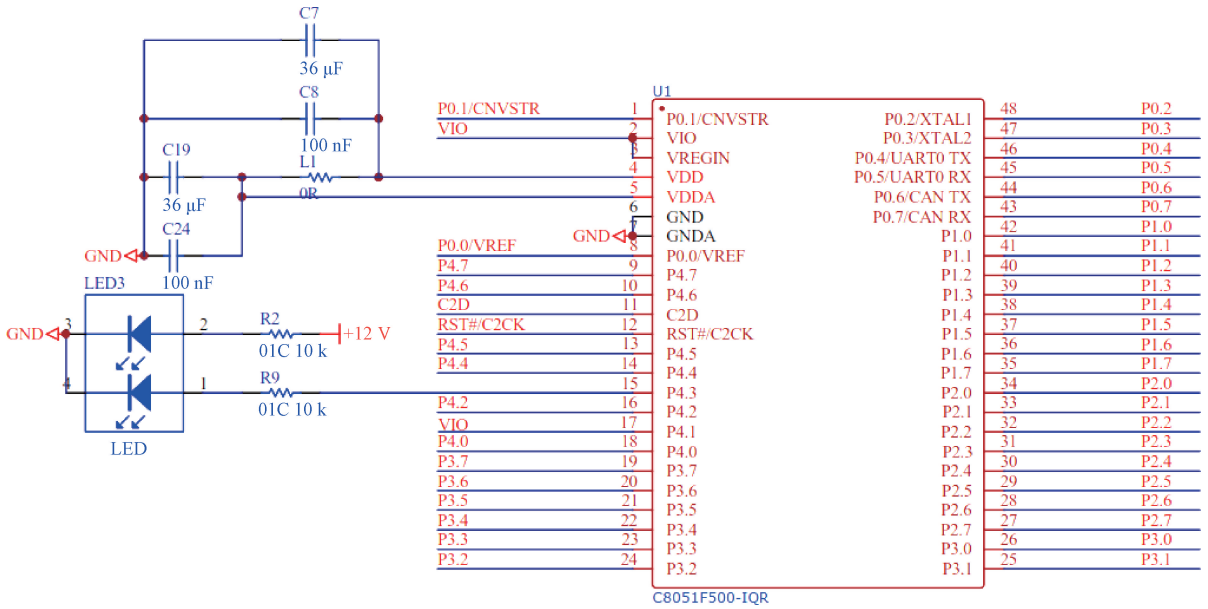


Fig. 15 C8051F500 single-chip microcomputer

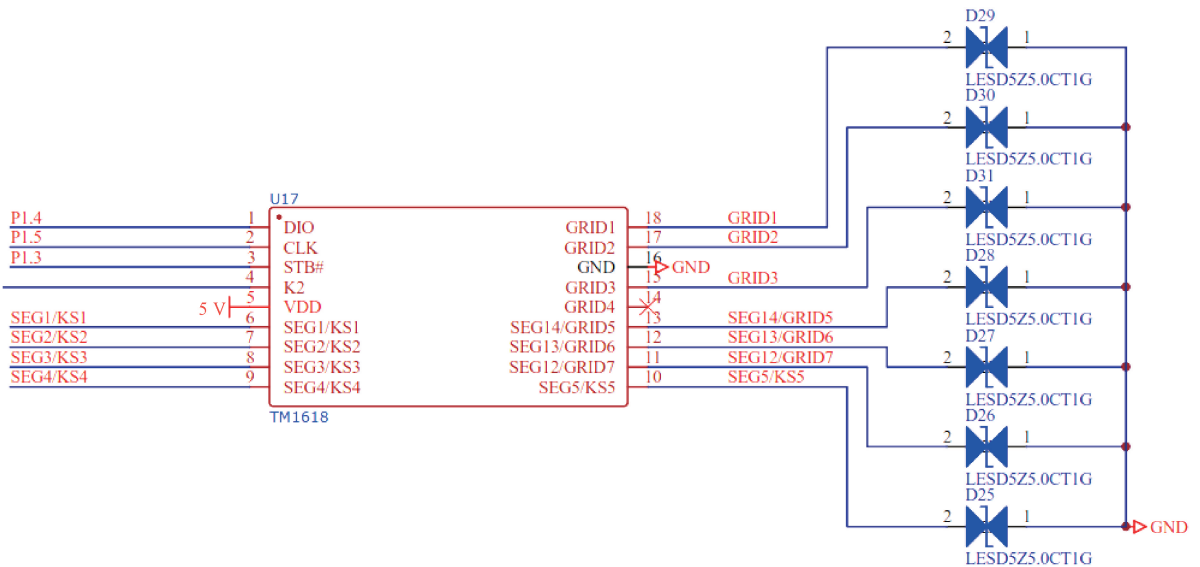


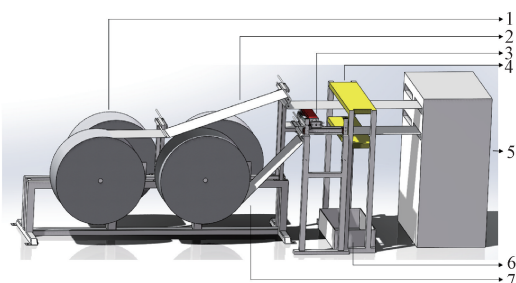
Fig. 16 TM1618 circuit

## 4 Equipment Design and Algorithms

### 4.1 Overall equipment design

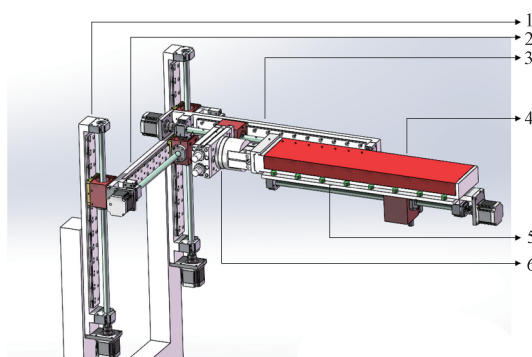
The intelligent metal detection and disposal automation equipment based on the geometric optimization driving algorithm is composed of a coiling device, metal detection and cutting devices, a metal impurity collecting device and a crusher room. The overall equipment design diagram is shown in Fig. 17. The metal detection device is composed of motion devices, a metal detection area, an LED indication area

and a flipping device, as shown in Fig. 18. The detection coils in the metal detection area are arranged in three coil combinations. The metal cutting device is installed on the back of the metal detection area and composed of a punching device, a punching bottom plate and a Y-axis motion device, as shown in Fig. 19. The stepping motor and the single-axis module can control the metal detection device and the metal cutting device to move freely along the X axis, the Y axis and the Z axis, and the flipping device can rotate 180° to realize the fast switching between the metal detection device and the punching device.



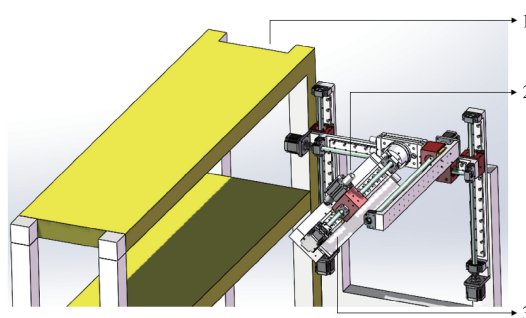
1—Coiling device; 2—wood pulp roll-up; 3—metal detection and cutting devices; 4—punching bottom plate; 5—crusher room; 6—metal impurity collecting device; 7—wood pulp roll-down.

Fig. 17 Overall equipment design diagram



1—Z-axis motion device; 2—X-axis motion device;  
3—Y-axis motion device; 4—metal detection area;  
5—LED indication area; 6—flipping device.

Fig. 18 Metal detection device diagram



1—Punching bottom plate; 2—punching device;  
3—Y-axis motion device.

Fig. 19 Metal cutting device diagram

The width of the wood pulp roll is 48 cm, the thickness is 1.5 mm, and the mass is 760 g. After the roll device is introduced, it is fed into the crusher room, and the conveyor line speed is 11–16 m/min. Among them, upper and lower rolls are alternately fed. When the photoelectric device detects that the wood pulp fed between the upper roll and the lower roll is about to run out, the upper/lower roll of the wood pulp starts to slow down until its speed is 0. At the same time, the lower/upper roll of the wood pulp gradually accelerates from the static state to the maximum speed, so as to ensure a constant amount of wood pulp feed and ensure the normal

operation of the subsequent production process.

If the wood pulp roll contains metal impurities, the magnetic field of the detection coil inside the metal detection area will change when it is introduced from the coiling device to the metal detection device. The LED light brightens, and the metal coordinates are initially positioned. At the same time, the main control chip issues a command, and the wood pulp roll slows down and stops. The metal detection device moves along the  $X$  axis to the re-inspection area, and moves freely in the  $X$  axis and the  $Y$  axis to perform the secondary detection of the wood pulp roll. By analyzing the signal waveforms of 24 detection coils, the system can accurately locate the metal coordinates if the signal peak exceeds the set threshold. According to the geometric optimization driving algorithm, the center position of the metal impurity and the final cutting area can be determined. The metal detection area is flipped by  $180^\circ$ . The punching device cuts all the metal impurities in turn, and the wood pulp roll containing metal impurities automatically enters the collection device. At the same time, the metal detection device moves back to the initial inspection area along the  $X$  axis. While cutting the upper/lower roll of the wood pulp containing metal impurities, the main control chip issues a command to control the motor to start upper and lower roll change functions, and the lower/upper roll of the wood pulp is accelerated to avoid shutdown and improve the production efficiency.

#### 4.2 Metal detection and cutting

The metal detection and cutting process of the wood pulp roll-up is shown in Fig. 20. The upper roll of wood pulp is transported to the crusher room at a normal working speed. The metal detection device is initially located in the initial inspection area, moves up along the  $Z$  axis, and is close to the upper roll of the wood pulp for detection, as shown in Fig. 21 (a). If metal impurities are detected, the LED light brightens, the upper roll of wood pulp slows down, and the metal detection device moves along the  $X$  axis to the re-inspection area, as shown in Fig. 21 (b). The metal detection device moves freely along the  $X$  axis and the  $Y$  axis in the re-inspection area, and performs multi-directional detection on the wood pulp roll. The signal waveforms of 24 detection coils are analyzed. If the signal peak exceeds the threshold  $k$ , the metal coordinates are determined. The metal detection device moves down along the  $Z$  axis and flips  $180^\circ$ , as shown in Fig. 21 (c). The punching device moves up to the position close to the upper roll of the wood pulp, as shown in Fig. 21 (d). According to the geometric optimization driving algorithm, the center of the metal impurity and the final cutting area can be determined. The punching device cuts all the detected metal impurities in turn and they enter the bottom collection device. The punching device moves down and flips  $180^\circ$ . The metal detection device moves back to the initial inspection area along the  $X$  axis, and the initial inspection and the re-inspection cycle operation are

carried out. At the same time, the wood pulp roll-up is accelerated to the working speed, and continues to be transported to the crusher room.

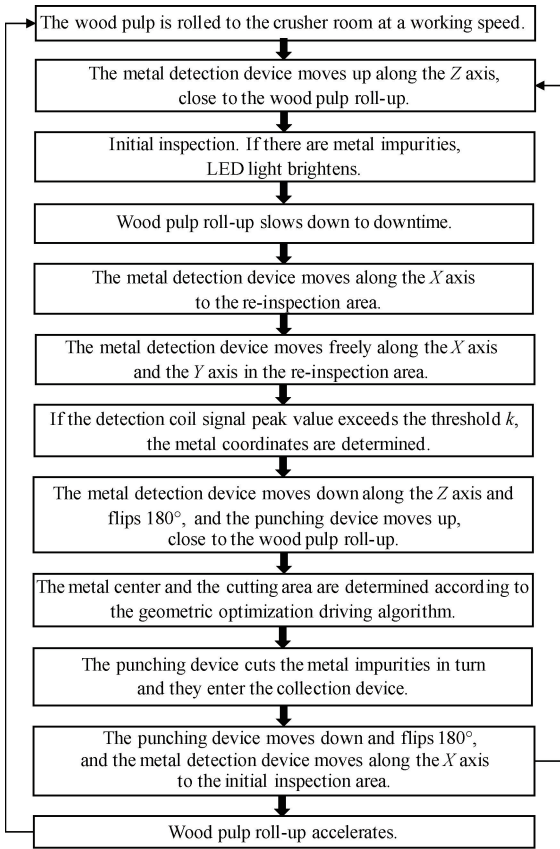


Fig. 20 Flow chart of metal detection and cutting of wood pulp roll-up

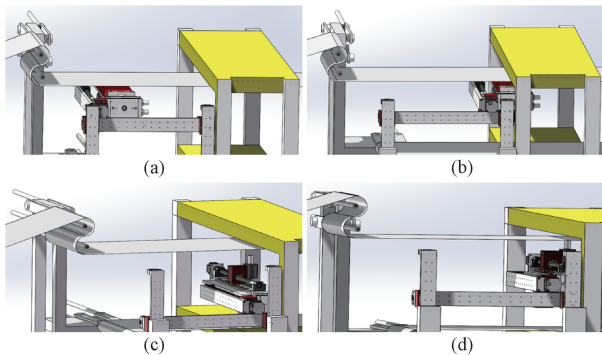


Fig. 21 Diagram of metal detection and cutting of wood pulp roll-up: (a) initial inspection area; (b) re-inspection area; (c) metal detection device after flipping; (d) punching device close to upper roll of wood pulp

When the metal detection device is turned 180° and the detection face is down, the metal detection of the wood pulp roll-down can be carried out. The metal detection and cutting process of the wood pulp roll-down is shown in Fig. 22. The lower roll of wood pulp is transported to the crusher room at a normal working speed. The metal detection device is located in the initial

inspection area, moves down along the Z axis, and is close to the lower roll of the wood pulp for detection, as shown in Fig. 23 (a). If metal impurities are detected, the LED light brightens, the lower roll of the wood pulp slows down, and the metal detection device moves along the X axis to the re-inspection area, as shown in Fig. 23 (b). The metal detection device moves freely along the X axis and the Y axis in the re-inspection area, and performs multi-directional detection on the wood pulp roll. The signal waveforms of 24 detection coils are analyzed. If the signal peak exceeds the threshold  $k$ , the metal coordinates are determined. The metal detection device moves up along the Z axis and flips 180°, as shown in Fig. 23 (c). The punching device moves down to the position close to the lower roll of the wood pulp, as shown in Fig. 23 (d). According to the geometric optimization driving algorithm, the center of the metal impurity and the final cutting area can be determined. The punching device cuts all the detected metal impurities in turn and they enter the bottom collection device. The punching device moves up and flips 180°. The metal detection device moves back to the initial inspection area along the X axis, and the initial inspection and re-inspection cycle operation are carried out. At the same time, the wood pulp roll-down is accelerated to the working speed, and continues to be transported to the crusher room.

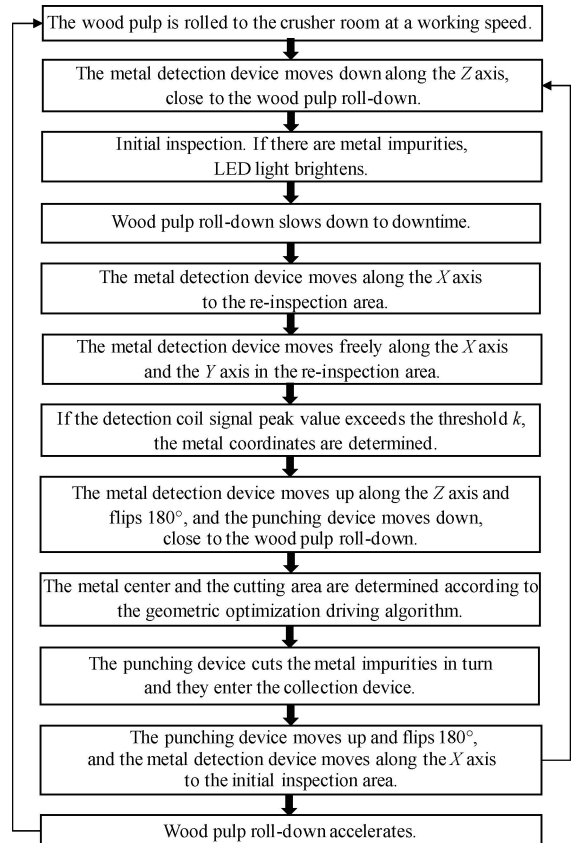


Fig. 22 Flow chart of metal detection and cutting of wood pulp roll-down

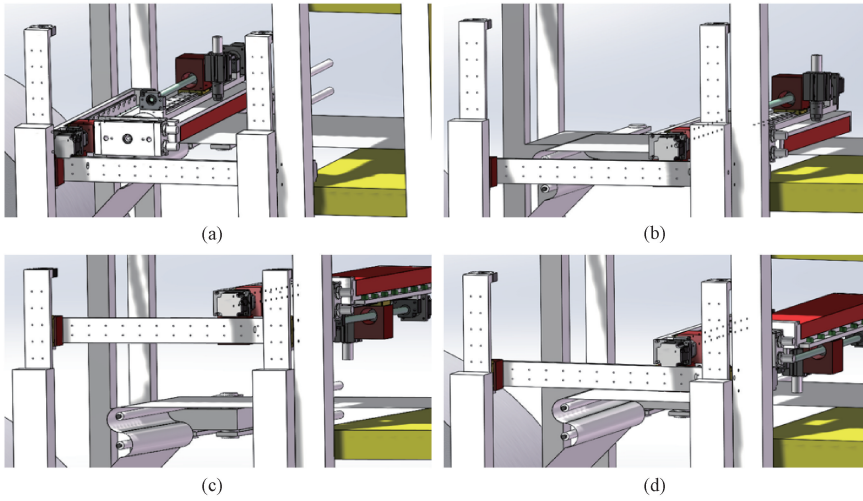


Fig. 23 Diagram of metal detection and cutting of wood pulp roll-down: (a) initial inspection area; (b) re-inspection area; (c) metal detection device after flipping; (d) punching device close to lower roll of wood pulp

### 4.3 Metal coordinate positioning and geometric optimization driving algorithm

#### 4.3.1 Metal coordinate positioning

The metal detection device detects metal impurities by generating a changing magnetic field. When a metal impurity enters the magnetic field generated by the coil, the total magnetic flux in the coil will change due to the eddy current effect, thereby changing the impedance of the coil. This change in the impedance affects the current passing through the coil, creating a measurable voltage change. If the peak value of the signal waveform exceeds a specific threshold, there may be a metal impurity under the coil.

In the initial inspection stage, the main task of the metal detection device is to quickly identify the possible areas of metal impurities. When the metal is detected, the LED light brightens and triggers the pulp roll to slow down and stop, sending it into the re-inspection area. Assume that the movement speed of the wood pulp roll is  $v$ , and the time required for the LED light to brighten and stop after the metal signal is detected is  $t_{\text{delay}}$ . Considering the delay and the redundancy of the signal, the distance  $d$  from the initial inspection to the re-inspection area is

$$d = vt_{\text{delay}}. \quad (1)$$

In order to accurately locate the metal impurities, the response of each coil in the metal detection device is analyzed. The metal detection device is composed of two rows of coils, 12 in each row. The arrangement makes it possible to cover the width of the detection area and accurately detect the position of the metal impurities.

The calculation of the coil coordinates takes into account the initial position of the metal detection device  $d_0$ , the moving speed  $v$ , the running time  $t$  and the radius  $r_0$  of the coil.

For the upper coil ( $i = 1, 2, \dots, 12$ ), the coordinates are defined as:

$$x_i = d_0 + vt, \quad (2)$$

$$y_i = 2r_0i - r_0. \quad (3)$$

For the lower coil ( $i = 13, 14, \dots, 24$ ), the coordinates are defined as:

$$x_i = d_0 + vt + r_0, \quad (4)$$

$$y_i = 2r_0i. \quad (5)$$

When the signal waveform peaks of any two coils  $P_i(x_i, y_i)$  and  $P_j(x_j, y_j)$  exceed the threshold, if their spatial distance satisfies certain conditions, they can be considered to detect the same metal impurity. In this case, only the position with a larger peak value is retained as the coordinates of the metal impurity. The determination condition is

$$\sqrt{(x_i - x_j)^2 + (y_i - y_j)^2} < r_0. \quad (6)$$

#### 4.3.2 Geometric optimization driving algorithm

In order to effectively remove metal impurities from materials, this study proposes an optimization algorithm based on scanning lines with a time complexity of  $O(n^2 \log_2 n)$ . The algorithm aims to identify the circular area that covers the most metal impurities and perform clipping on this basis to improve material utilization and preserve edge integrity.

##### 1) Determination of the metal impurity center

For each metal impurity  $P_i(x_i, y_i)$ , a circle with  $P_i$  as the center and  $R$  as the radius is established. Any point  $Q(x, y)$  covered by this circle satisfies the following condition:

$$\sqrt{(x - x_i)^2 + (y - y_i)^2} \leq R. \quad (7)$$

For all points  $P_i$  whose distance from the edge of the cloth is higher than  $D_{\text{edge}}$ , the above steps are performed to accumulate the count of the number of times each point  $Q$  is covered.  $D_{\text{edge}}$  is generally set to

twice the size of  $R$ .

## 2) Determination of the cutting area

Traverse all points  $Q(x, y)$  to find the point with the largest count. Taking this point as the center of the circle and  $R$  as the radius, the cutting area is determined. After the clipping is performed, the corresponding count value is updated for each impurity  $P_i$  in the clipped area.

## 3) Iterative clipping

Repeat step 2) until all metal impurities with a diameter larger than  $D_{\text{edge}}$  at the edge of the cloth are cut. For the metal impurities in the edge of the cloth, the same method is used for processing, and the points with the farthest distance from the edge and a larger count are preferentially cut.

The count function  $N(Q)$  for the point  $Q(x, y)$  is defined as

$$N(Q) = \sum_{i=1}^n I \sqrt{(x - x_i)^2 + (y - y_i)^2} \leq R, \quad (8)$$

where  $I(\cdot)$  is an indicator function. When the condition is satisfied,  $I(\cdot)$  is 1; otherwise, it is 0.

The clipping decision is based on maximizing  $N(Q)$ :

$$Q_{\max} = \arg \max_{Q(x,y)} N(Q). \quad (9)$$

Then, the clipping is performed with  $Q_{\max}$  as the center and  $R$  as the radius.

Through the above algorithm, the cutting area can be efficiently determined to maximize the metal impurity coverage and minimize the material loss, especially in retaining the edge of the material.

## 4.4 Up and down roll switching strategy and speed compensation algorithm

In the workflow of the automated production line, the setting strategy of upper and lower rolls can realize the rapid switching of the roll material without stopping the machine when the metal impurities are detected, so as to maintain continuous production and maximize the production efficiency.

Specifically, when the detection system detects metal impurities in the upper roll, the system will immediately switch to the lower roll for feeding, while the upper roll suspends the supply and performs the removal of metal impurities. After elimination, the supply of the roll is restored, which ensures the continuous operation of the production line. However, the operation of removing metal impurities will lead to a

loss of the cloth area. In order to compensate for this loss, this study proposes a speed compensation algorithm.

Assume that the width of the wood pulp roll is  $w$ , the original feed speed of the wood pulp roll is  $v_{\text{ori}}$ , and the area of the wood pulp roll passing through per second is  $v_{\text{ori}} w$ . In order to compensate for the area  $A$  of the removal loss, it is necessary to feed an additional amount of the cloth within the compensation time  $t$ . Therefore, the increasing speed  $\Delta v$  is

$$\Delta v = A / (t \times w). \quad (10)$$

Therefore, the feed speed after compensation  $v_{\text{com}}$  should be adjusted to

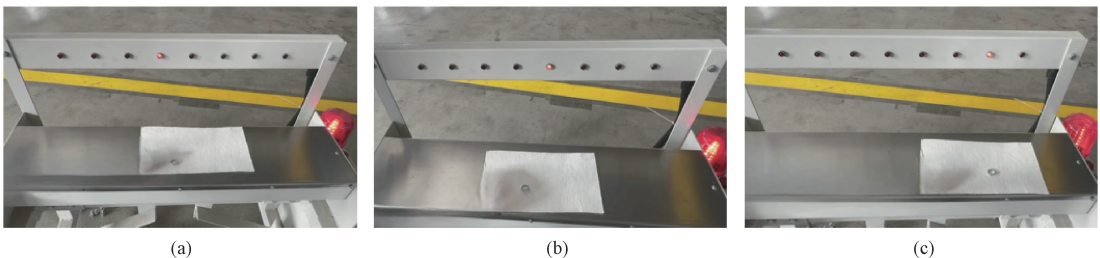
$$v_{\text{com}} = v_{\text{ori}} + \Delta v. \quad (11)$$

In this way, the production line can eliminate metal impurities and adjust the feed speed to compensate for the loss of cloth caused by the rejection operation, ensuring the production efficiency and the effective use of materials. This speed compensation strategy provides an efficient and practical solution for the treatment of metal impurities in the automated assembly line.

## 5 Experimental Result Analysis

Due to the confidentiality of the actual production line, a prototype was built to test the metal detection sensitivity. The steel ring with a diameter of 16 mm, the steel ring with a diameter of 8 mm, and the steel needle with a length of 20 mm and a thickness of 0.8 mm were tested, respectively. They passed through eight detection areas in turn to observe whether the LED light brightens at the corresponding positions were on. The test results are shown in Fig. 24.

It can be seen from Fig. 24 that when the steel ring with a diameter of 16 mm, the steel ring with a diameter of 8 mm, and the steel needle with a length of 20 mm and a thickness of 0.8 mm pass through eight detection areas in turn, the LED light brightens at the corresponding positions, suggesting that metal impurities are detected. However, there are also cases where the position of the LED light is not corresponding to the detection area where the metal is located, suggesting that the metal detection sensitivity is not 100% accurate. By analyzing all the test results, the metal detection sensitivity can reach more than 95%.



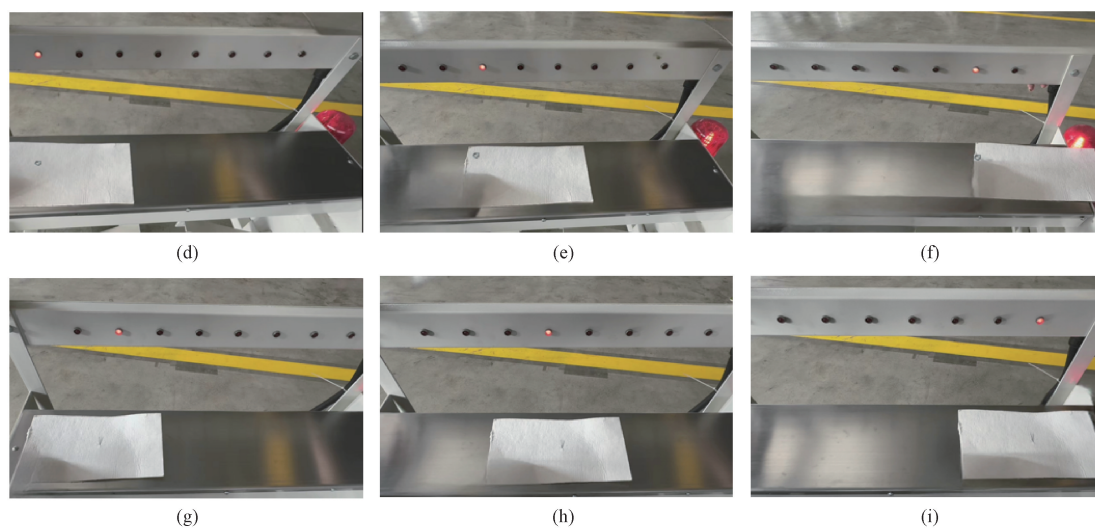


Fig. 24 Metal detection sensitivity test results: (a)–(c) steel ring with a diameter of 16 mm; (d)–(f) steel ring with a diameter of 8 mm; (g)–(i) steel needle with a length of 20 mm and a thickness of 0.8 mm

## 6 Conclusions

In this paper, an intelligent metal detection and disposal automation equipment based on the geometric optimization driving algorithm is designed. Eddy current sensors and self-oscillating detection circuits are applied, and the arrangement of detection coils is optimized. The arrangement of three coil combinations can effectively improve the speed of metal detection. Through a series of circuit design, the metal detection sensitivity is improved, more than 95%, and the sensitivity can be adjusted according to the needs of the production line, and the LED light is driven to realize the initial positioning of the metal impurity. The metal detection device moves freely in the  $X$  axis and the  $Y$  axis, and performs multi-directional secondary detection on the wood pulp roll. By analyzing the signal waveform of the detection coil, when the signal peak exceeds the threshold, the precise positioning of the metal impurity coordinates is realized.

Based on the geometric optimization driving algorithm, the cutting area is determined by locating the center of the circle that covers the maximum area, aiming to minimize the cutting area while maximizing material usage. This methodology is integrated into the process of determining the center coordinates of the metal impurities and the final cutting area. The punching device then sequentially cuts them to further reduce the cutting area and minimize the material waste. Additionally, by employing the farthest edge covering circle algorithm, the method strives to preserve as many materials at the edges as possible, enhancing the efficiency of material usage.

Furthermore, based on the speed compensation algorithm, the flexible switching of the upper and lower wood pulp rolls is realized. This ensures the accurate removal of metal impurities while maintaining the normal

operation of the subsequent process and maximizing the production efficiency.

In summary, compared with the existing production line metal detection device, the designed intelligent metal detection and disposal automation equipment, enhanced with the geometric optimization driving algorithm, possesses higher detection sensitivity, more precise metal coordinates positioning, a smaller cutting material area and a higher production efficiency. Moreover, by minimizing the edge damage and preserving more material at the edges, it ensures that there are no issues during edge transportation with the roller. It is anticipated to be applied to actual production, enhancing the entire production process's continuity, automation and intelligence.

## References

- [ 1 ] CAMPILHO R D S G, SILVA F J G. Industrial process improvement by automation and robotics [J]. *Machines*, 2023, 11(11): 1011.
- [ 2 ] DZEDZICKIS A, SUBAČIŪTĖ-ŽEMAITIENĖ J, ŠUTINYS E, et al. Advanced applications of industrial robotics: new trends and possibilities [J]. *Applied Sciences*, 2021, 12(1): 135.
- [ 3 ] LV T, HAN N. Intelligent manufacturing: global trends and China's strategy [J]. *Frontiers*, 2015 (11): 6-17. (in Chinese)
- [ 4 ] ZHANG S. Industry 4.0 and intelligent manufacturing [J]. *Mechanical Design and Manufacturing Engineering*, 2014, 43(8): 1-5.
- [ 5 ] LI C Z, WEI K H, ZHAO Y B, et al. Improvement of high-speed detection algorithm for nonwoven material defects based on machine vision [J]. *Journal of Donghua University (English Edition)*, 2024, 41(4): 416-427.
- [ 6 ] XUE Z. Based on the application and research of

- magnetic anomaly signal detection technology in the field of metal detection[D]. Xi'an: Chang'an University, 2021. (in Chinese)
- [7] YANG Y, WANG G, TONG Y, et al. Determination of 10 metal elements in soil by X-ray fluorescence spectrometry [J]. *Leather Production and Environmental Protection Technology*, 2022, 3(11): 60-63.
- [8] JIANG H, CHEN J Q, DENG J H, et al. Quantitative determination of heavy metal Pb content in soybean oil based on microwave detection technique combined with multivariate analysis[J]. *Sensors and Actuators A: Physical*, 2023, 363: 114771.
- [9] QIAN B Y, MOU L, WU L, et al. A direction-sensitive microwave sensor for metal crack detection [J]. *Applied Sciences*, 2022, 12(18): 9045.
- [10] SI D P. Metal detectors [J]. *Modern Physics*, 2006(4): 37-39.
- [11] DU Y Y, CHEN K X, CHEN Y Q, et al. Realization method of current waveform of GMAW magnetron power supply based on RLC series resonance [J]. *Hot Processing Technology*, 2023, 52(3): 120-123, 131.
- [12] ZHAI W M. Research on metal detector based on magnetoresistance sensor array [D]. Harbin: Harbin Engineering University, 2022. (in Chinese)
- [13] WU X Q. Research on metal detector sensor based on closed circular coil system [D]. Hefei: Anhui University, 2016. (in Chinese)
- [14] ZHANG H Z, LI S C. Design and implementation of audio signal amplification based on digital logic circuits [J]. *Modern Computer*, 2022, 28(9): 118-120.
- [15] SUN Z P, GUAN Y C, HE J, et al. Research and design of fiber grating demodulation circuit based on fan blade stress monitoring [J]. *Modern Information Technology*, 2023, 7(8): 171-174.
- [16] XU H X, CHI X L. Design of demo system based on C8051F500 microcontroller [J]. *Microprocessor*, 2023, 44(3): 57-61.

## 基于几何优化驱动算法的智能金属探测及处置自动化装备

田雪慧, 李成族, 位珂晗, 钱洋, 张璐, 王荣武\*  
 东华大学 纺织学院, 上海 201620

**摘要:** 为解决木浆非织造原料生产线混入金属杂质的问题, 设计了一款智能金属探测及处置自动化装备。基于电磁感应原理, 采用初检加多方位复检的方式, 实现对金属坐标的精准定位。基于几何优化驱动算法, 通过找到最多覆盖圆的圆心所在位置来判定裁剪区域。该算法可极大程度地缩小裁剪面积, 并通过边缘最远覆盖圆算法, 尽可能保留边缘布料。基于速度补偿算法, 可实现上下卷的灵活切换以保证生产效率最大化。与现有生产线的金属检测装置相比, 所设计的自动化装备具有检测灵敏度更高、金属位置定位更精准、裁剪物料面积更小、生产效率更高的优势, 可以使生产流程更连续化、自动化和智能化。

**关键词:** 智能制造; 电磁感应; 金属探测; 几何优化驱动算法; 自动化装备